

Na⁺,K⁺-ATPase Pump Currents in Giant Excised Patches Activated by an ATP Concentration Jump

Thomas Friedrich, Ernst Bamberg, and Georg Nagel

Max-Planck-Institut für Biophysik, Kennedyallee 70, D-60596 Frankfurt am Main, Germany

ABSTRACT The giant-patch technique was used to study the Na⁺,K⁺-ATPase in excised patches from rat or guinea pig ventricular myocytes. Na⁺,K⁺-pump currents showed a saturable ATP dependence with a K_m of $\sim 150 \mu\text{M}$ at 24°C. The pump current can be completely abolished by ortho-vanadate. Dissociation of vanadate from the enzyme in the absence of extracellular Na⁺ was slow, with a k_{off} of $3 \cdot 10^{-4} \text{ s}^{-1}$ ($K_i \approx 0.5 \mu\text{M}$, at 24°C). Stationary currents were markedly dependent on intracellular pH, with a maximum at pH 7.9. Temperature-dependence measurements of the stationary pump current yielded an activation energy of $\sim 100 \text{ kJ mol}^{-1}$. Partial reactions in the transport cycle were investigated by generating ATP concentration jumps through photolytic release of ATP from caged ATP at pH 7.4 and 6.3. Transient outward currents were obtained at pH 6.3 with a fast rising phase followed by a slower decay to a stationary current. It was concluded that the fast rate constant of $\sim 200 \text{ s}^{-1}$ at 24°C (pH 6.3) reflects a step rate-limiting the electrogenic Na⁺ release. Simulating the data with a simple three-state model enabled us to estimate the turnover rate under saturating substrate concentrations, yielding rates (at pH 7.4) of $\sim 60 \text{ s}^{-1}$ and 200 s^{-1} at 24°C and 36°C, respectively.

INTRODUCTION

The Na⁺,K⁺-ATPase (or sodium pump) is an essential enzyme found in virtually every animal plasma membrane. Because this enzyme expels three Na⁺ ions from the cell in exchange for two K⁺ ions per ATP hydrolyzed (for review see Läger, 1991, and Glynn, 1993), it generates an electric current and its activity can be directly monitored by measuring this current. Several organs, like kidney, heart, and nervous tissue, contain a very high density of Na⁺,K⁺-ATPase, and these sources have been frequently used for studying the sodium pump's reaction cycle. Because three α -isoforms are differentially expressed in different tissues (Sweadner, 1989; Lingrel, 1992) and different species were used, investigations on Na⁺,K⁺-ATPase have in fact been done with enzymes of quite different primary structure. Nevertheless, remarkable similarity was found in studies on different enzyme sources and wide agreement has been reached upon the basic validity of the Albers-Post model (Fahn et al., 1966; Post et al., 1969) to explain ion pumping by the Na⁺,K⁺-ATPase.

In our patch clamp study we used the giant-patch technique to record current through the excised plasma membrane patches of isolated ventricular myocytes from rat or guinea pig. Cardiac myocytes proved to be an excellent system for the electrophysiological investigation of the

Na⁺,K⁺-ATPase, yielding valuable new insight into the voltage dependence of the overall transport and of partial reactions (e.g., Nakao and Gadsby, 1986; Gadsby and Nakao, 1989; Hilgemann, 1994). With the advent of the giant-patch technique (Hilgemann, 1989, 1995a) it became possible to study the Na⁺,K⁺-ATPase from heart plasma membrane under the more precisely controlled conditions of an excised patch (Hilgemann et al., 1991; Collins et al., 1992; Hilgemann, 1994).

The caged-ATP technique provided insight in the Na⁺ translocating step of the Na⁺,K⁺-ATPase reaction cycle in experiments with right-side-out vesicles (Forbush, 1984) or with membrane fragments attached to a black lipid membrane (BLM). The BLM experiments with purified enzyme from pig or rabbit kidney or eel electroplax (Fendler et al., 1985, 1987, 1993; Nagel et al., 1987; Borlinghaus et al., 1987; Wuddel and Apell, 1995), because of a high signal to noise ratio, allowed detailed analysis of the partial reactions yielding rate constants for the electrogenic Na⁺ transport step. A disadvantage was the capacitive (AC-) coupling of the membrane fragments to the BLM, which does not allow exact voltage control or the direct recording of a steady-state electrical current.

In the first part of this article we characterize the pump current that can be measured in giant excised patches by bath solution changes between ATP-free and ATP-containing solutions. The ultimate goal of our study, however, was to apply the technique of a fast ATP concentration jump via photolysis of caged ATP (Kaplan et al., 1978) directly at a giant patch from heart cells. The giant-patch technique in combination with photolysis of caged ATP has the advantage of controlling membrane potential and substrate concentration on both sides of the membrane and of allowing a direct, time-resolved measurement (DC-coupled) of the ATP jump-induced current. In the second part we will show that the rate-limiting step in the Na⁺ transport limb, if

Received for publication 25 April 1996 and in final form 10 September 1996.

Address reprint requests to Dr. Georg Nagel, Max-Planck-Institut für Biophysik, Kennedyallee 70, D-60596 Frankfurt, Germany. Tel.: 49-69-6303-303; Fax: 49-69-6303-305; E-mail: nagel@kennedy.mpibp.uni-frankfurt.de.

Part of this work was presented at the 39th Annual Meeting of the Biophysical Society and published in abstract form (Friedrich and Nagel, 1995).

© 1996 by the Biophysical Society

0006-3495/96/11/2486/15 \$2.00

measured under appropriate conditions, appears electrogenic with a rate constant of 200 s^{-1} at 24°C , confirming earlier work on pig kidney and eel electroplax Na^+, K^+ -ATPase adsorbed to a BLM (Fendler et al., 1987, 1993). This conclusion is in contrast to a postulated rate of $\sim 25 \text{ s}^{-1}$ at 22°C (Borlinghaus et al., 1987; Wuddel and Apell, 1995), derived from BLM experiments with caged ATP, but not contradictory to an ultrafast electrogenic release of Na^+ (Gadsby et al., 1993; Hilgemann, 1994; Wagg et al., 1996), if preceded by an (electrogenic or electroneutral) step with a rate of 200 s^{-1} , as this is kinetically equivalent.

MATERIALS AND METHODS

Cell-preparation

Ventricular myocytes from rat or guinea pig were isolated according to established procedures (Isenberg and Klöckner, 1982; Collins et al., 1992). Briefly, cells were obtained by retrograde perfusion of the heart on a Langendorf-type apparatus in which continuous solution flow was maintained by a peristaltic pump. Hearts were digested using a low- Ca^{2+} Tyrode's solution containing collagenase (Sigma type 1 or Worthington, 1 mg/ml) followed by dispersion with scissors and filtering through nylon mesh. Cells were stored (up to 3 days) in a K^+ -rich, Ca^{2+} -free solution at $+4^\circ\text{C}$ (Storage DS or TS, see below), in which they formed spherical membrane protrusions or blebs, comprised of plasma membrane (Collins et al., 1992). These blebs were used to form gigaohm seals with the patch pipette.

Pipettes for giant excised patches

Pipettes were pulled from borosilicate glass capillaries (1.6 mm ID, 2.2 mm OD, Type N-51 A, Drummond Scientific Co., Broomall, PA) on a conventional two stage puller (PP-83, Narishige, Tokyo, Japan), yielding tip openings between 20 and $26 \mu\text{m}$. Pipette tips were briefly heat polished and immersed into D,L- α -tocopherol-acetate immediately before use to improve the quality of the seal. Alternatively, a hydrocarbon mixture of light and heavy mineral oil (Sigma) together with parafilm as described by Hilgemann and co-workers (Collins et al., 1992) was used for hydrophobic coating of the patch pipette.

Experimental solutions

Tyrode for myocyte preparation: 130 mM NaCl, 5.4 mM KCl, 0.3 mM $\text{NaH}_2\text{PO}_4 \cdot 2\text{H}_2\text{O}$, 1 mM MgCl_2 , 20 mM taurine, 5 mM creatine, 10 mM HEPES, 11 mM glucose, $36 \mu\text{M}$ CaCl_2 , pH 7.35 with NaOH.

Storage solution DS: 134 mM KCl, 10 mM EGTA, 10 mM HEPES, 10 mM glucose, 2 mM MgCl_2 , pH 7.4 with KOH, used for storage of guinea pig myocytes.

Storage solution TS: 70 mM KOH, 50 mM glutamic acid, 40 mM KCl, 20 mM taurine, 20 mM KH_2PO_4 , 3 mM MgCl_2 , 0.5 mM EGTA, 10 mM HEPES, pH 7.4 with KOH, used for storage of rat myocytes.

Bath solutions

B-F: Bath solution for continuous flow fast solution exchange experiments contained (in mM): 40 NaCl, 100 *N*-methyl-D-glucamine (NMG), 10 EGTA, 10 HEPES (for pH 7.4) or MES (for pH 6.3), 20 tetraethylammonium chloride, 2 MgCl_2 , pH 7.4 or 6.3 adjusted with HCl. For Na^+ -dependence measurements, solutions containing either 140 mM NaCl or 140 mM NMG-Cl and the rest of the above were mixed to obtain the desired concentration of Na^+ .

B-pH: For pH-dependence measurements 10 mM MES and 10 mM Tris were added in addition to 10 mM HEPES; pH was adjusted to the stated values adding HCl.

To test Na^+, K^+ -ATPase activity, MgATP (Sigma, from equine muscle, vanadate-free) was added to B-F or B-pH usually at a concentration of $500 \mu\text{M}$.

B-P: Bath solutions for caged-ATP photolysis at pH 6.3 or 7.4 contained (in mM): 40 NaCl, 100 NMG, 10 MES (for pH 6.3) or HEPES (for pH 7.4), 10 EGTA, 20 tetraethylammonium chloride, and 2 MgCl_2 , pH adjusted with HCl. 1 mM glutathione or 1 mM L-ascorbic acid were also added. 10 units/ml hexokinase (Sigma, München, Germany) together with 1 mM glucose were added, because caged-ATP stock solutions usually contain 0.5% of free ATP. Caged ATP (P^3 -1-(2-nitro)phenylethyladenosine-5'-triphosphate, triethylammonium salt) was used in concentrations from 10 to $500 \mu\text{M}$. It was synthesized as described previously (Fendler et al., 1985).

Pipette solutions

Three different pipette solutions were used, containing (in mM):

P-Na-K: 145 NaCl, 10 HEPES, 5 KCl, 2 BaCl_2 , 2 MgCl_2 , 0.5 CdCl_2 , adjusted to pH 7.4 with NaOH.

P-NMG-K: 145 NMG, 10 HEPES, 5 KCl, 2 BaCl_2 , 2 MgCl_2 , 0.5 CdCl_2 , adjusted to pH 7.4 with HCl.

P-NMG-Cs: 1 mM CsCl was used instead of 5 mM KCl in the P-NMG-K solution in a few experiments.

All chemicals were of analytical or higher grade (Merck, Darmstadt, Germany).

Electrical recording in the perfusion and photolysis chamber

The myocytes were suspended in a glass petri dish of 35-mm diameter, which was mounted on an inverted microscope (Zeiss axiovert 35 M, Carl Zeiss, Oberkochen, Germany). Gigaohm seals were obtained on "blebs" from myocytes after switching the pressure applied to the pipette solution from moderate overpressure to zero (or slight suction if necessary), as described (Collins et al., 1992). After excision of the patch, the pipette was moved into the temperature-controlled perfusion and photolysis chamber.

Patch currents were measured at 0 mV using an Axopatch 200 A amplifier (Axon Inst., Foster City, CA), using capacitive feedback for low noise recording. Current and solution exchanges were routinely recorded continuously at low resolution (10 Hz) on a chart recorder (e.g., Fig. 2) and at 50 Hz (Figs. 3 A, 4 A, 5 A, 6 A, and 9) on the hard disc of a personal computer using KAN1 software (MFK, Niedernhausen, Germany). Time-resolved currents from photolysis experiments were usually filtered at 2 kHz and stored on an additional personal computer using PClamp 6 software (Axon Inst., Foster City, CA), which also controlled laser pulses or electric valve switching. To detect possible conductivity changes of the membrane due to irradiation with ultraviolet (UV) light (which would alter the current amplitude in case of incomplete compensation of pipette potential) a 5-mV test pulse was applied before and after the flash to check membrane resistance. Traces with a flash-induced conductivity change were rejected.

The temperature-controlled perfusion chamber is shown in Fig. 1. Its small volume (10–20 μl) allowed solution exchange within seconds (being 80% complete after 1 s) as can be seen from the decay of the pump current upon ATP withdrawal (e.g., Figs. 2, 3 A, 5 A). The perfusion chamber consisted of a $1 \times 1 \times 1$ -cm brass cube (Fig. 1 a), which was carefully coated for electrical isolation. A duct was drilled into the cube for circulating liquid from a temperature controlled water bath (not included in Fig. 1 for clarity). Bath solution flow was controlled by electric valves (General Valves, Fairfield, NJ). Eight different bath solutions were water-jacketed by the same water bath before entering the solution inflow line (Fig. 1 c). The dead volume after a solution switch consisted of only a few microliters within that common line. To measure temperature in close vicinity to the

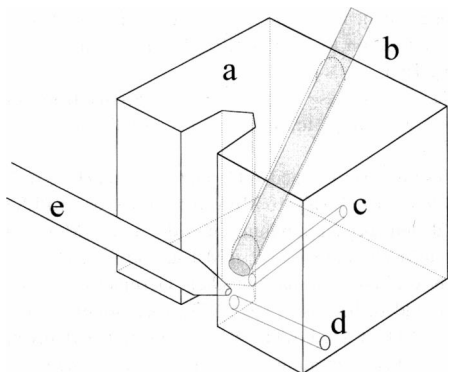


FIGURE 1 Schematic view of the temperature-controlled perfusion chamber: brass cube (a) with quartz-fiber (b) into which the laser flash is sent, solution inflow line (c) for eight different solutions, and the hole for temperature sensor (d). An additional duct is drilled into the brass cube to water-jacket the perfusion chamber (not included in the figure for clarity). Also shown is a patch-pipette (e), drawing not to scale; brass cube = 10 mm \times 10 mm \times 10 mm.

patch membrane, the sensing wire of a digital thermometer was fed through a tiny hole in the brass cube (Fig. 1 d) into the solution exchange chamber. Temperatures measured there were taken as the patch temperature (see Fig. 6 A) and deviated by a maximum of 1 K from the temperature in the water bath at extreme temperatures (9°C or 39°C). The end of a fused-silica light guide was mounted within the perfusion chamber through an additional duct (Fig. 1 b). The patch pipette was placed as close as possible to the end of the light guide, up to a distance of ~ 100 μ m. Ten-nanosecond UV-light flashes from an excimer laser of 308-nm wavelength (Lambda Physik, Göttingen, Germany) were sent into the light guide with energy densities between 14 and 180 mJ/cm² (attenuated by neutral density filters). These conditions led to 3–30% liberation of ATP from caged ATP after a single flash. Most experiments were carried out in the above described temperature-controlled chamber, but some earlier experiments were done in a simpler chamber at room temperature, which was always recorded (22–27°C).

Stability of pump current during an experiment

It is known from patch-clamp studies in whole-cell experiments that the amplitude of the stationary Na⁺,K⁺-ATPase pump current decreases grad-

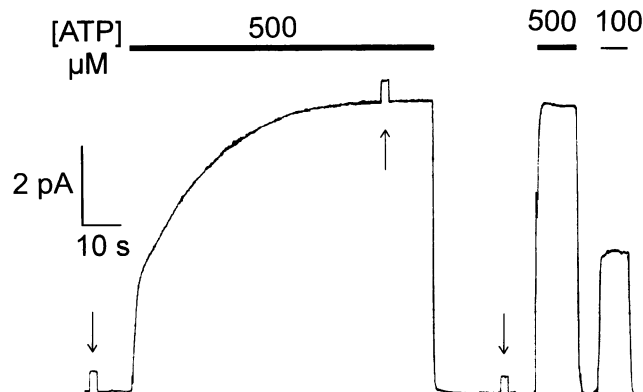


FIGURE 2 Slow activation of pump current upon first application of ATP. 10-mV pulses (indicated by arrows) were applied to test seal resistance (≈ 20 G Ω), remaining constant during the recording. Bath solution: B-F with 500 or 100 μ M MgATP, as indicated. Pipette solution: P-NMG-K. Rat cell, T = 24°C.

ually with time leading to a rundown to 50% within about half an hour (Gadsby and Nakao, 1989). In our giant-patch experiments, rundown (without caged-ATP photolysis, see below) was not that pronounced and pump currents remained remarkably constant. In some experiments a decrease to $\sim 80\%$ of the initial value occurred within 25 min.

When superfusion with a Na⁺- and ATP-containing solution was carried out for the first time after excision of the membrane patch, a slow increase in pump current could frequently be observed (see Fig. 2). A fast initial rise in pump current (due to the solution exchange) was followed by a slower rise to the final stationary value. Subsequent activations of the pump only led to a fast rise to the full activity within the typical time range of the solution exchange. This phenomenon was also described by Hilgemann (1995b).

The magnitude of the pump current obtained upon first application of ATP was ~ 30 –80% of the final value. The subsequent increase in pump current was slow so that it took ~ 1 min at 24°C to reach saturation. In agreement with Hilgemann's report (Hilgemann, 1995b) it was dependent on the presence of ATP but not on the overall pump activity, because a Na⁺-free ATP-containing solution could also lead to an increase in pump activity that only becomes apparent afterward when probed with Na⁺- and ATP-containing solution. In contrast, after superfusion with ATP-free solutions the pump activity (as revealed afterward) remained at a suboptimal level (data not shown). Therefore, ATP was always applied at the beginning of an experiment until the pump current became stable. To account for possible changes in the overall amplitude of the pump current, the experimental protocols were arranged in such a way that pump activity was monitored under reference conditions before and after a change of conditions, which were expected to influence activity (Na⁺-concentration, pH, for protocol arrangement see Fig. 3 A or 5 A).

Rundown of pump currents was significantly pronounced in experiments including caged-ATP photolysis (see Fig. 9). This effect can only be attributed to a minor extent to protein damage caused by irradiation with UV light of 308-nm wavelength. We observed that laser flashes (308 nm, 10 ns) caused a noticeable decrease in pump activity only if applied at energy densities much higher than those used for photolysis experiments. It was noticed a long time ago (Kaplan et al., 1978) that a by-product of the photolytic reaction, later identified as 2-nitrosoacetophenone, had harmful effects on Na⁺,K⁺-ATPase activity, but 2 mM glutathione was sufficient to prevent inhibition. After these results we added 1 mM glutathione to all of our samples, which had a maximal caged-ATP concentration of 500 μ M, but no significant protective action was observed. Other reducing agents like dithiothreitol and L-ascorbic-acid were tried but none led to a significant improvement. Addition of dithiothreitol led to destruction of the patch membrane within seconds. Investigations of the photolysis-induced inhibition revealed that repeated photolysis of caged ATP at high concentrations causes a decay of the stationary pump current without affecting the rate constants of the induced transient currents. This suggests that each flash leads to complete damage of a specific percentage of the transport molecules rather than to a modification of the whole ensemble's transport properties.

Data analysis

Steady-state kinetic data were obtained from measuring the amplitude of pump currents as the difference between currents in the presence and in the absence of ATP. The amplitudes were normalized with reference to values obtained under standard conditions of a specific experiment. If possible, measurements of pump currents under standard conditions were carried out in a "bracketing" manner, before and after a change of effector concentration, to account for possible changes in the overall amplitude of pump current (see above). If such a change occurred, an interpolated pump current value was taken as a reference.

The released fraction η of ATP from caged ATP after a laser flash was calculated according to the following equation:

$$\eta = 1 - e^{-\kappa E} \quad (1)$$

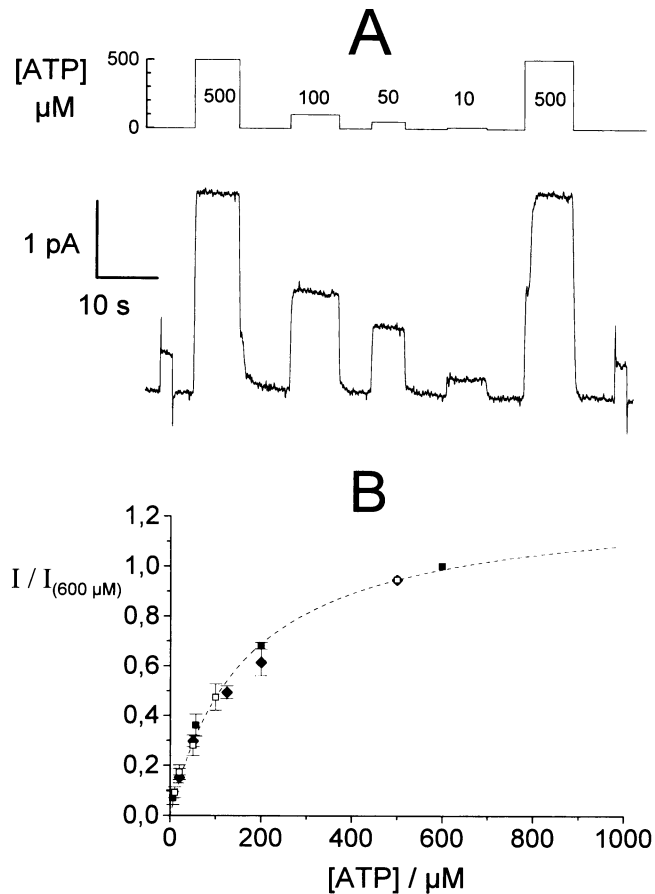


FIGURE 3 Recording of patch current in response to superfusion of the patch with solutions containing different MgATP concentrations as indicated in the upper part of A. At the beginning and the end of the current recording a 10-mV voltage pulse was applied to test the seal resistance ($\approx 20 \text{ G}\Omega$). Bath solution: B-F, pipette solution: P-NMG-K. Rat cell, $T = 24^\circ\text{C}$. (B) Dependence of the normalized patch current on ATP concentration, plotted are means \pm SD. (■) shows data from rat cell experiments with pipette solution P-NMG-Cs, (□) rat cell experiments with pipette solution P-NMG-K, and (◆) guinea pig cell experiments with pipette solution P-NMG-K. Included is a least-squares fit of a Michaelis-Menten equation to the data (■) (dashed line), leading to a V_{max} of 1.26 ± 0.06 (current at $500 \mu\text{M}$ ATP was set to 1.0), and an apparent K_m of $165 \pm 20 \mu\text{M}$. Apparent K_m for the rat cell experiments with P-NMG-K is $146 \pm 23 \mu\text{M}$ (□) and for guinea pig cell experiments with pipette solution P-NMG-K is $163 \pm 13 \mu\text{M}$ (◆). $T = 24^\circ\text{C}$.

where E is the energy density of the applied UV light flash (expressed in mJ/cm^2) at the end of the light guide and κ is an empirical constant, which was determined to be $0.002 \text{ cm}^2/\text{mJ}$ by means of a luciferin/luciferase assay (ATP-Biolumineszenz CLS, Boehringer, Mannheim, Germany).

Rate-constants from transient current measurements were calculated by using least-squares fitting of a model function to the data ($I_{(t)}$), which included a double exponential decay and a stationary component (program used for data analysis: ORIGIN, Microcal Software Inc., Northampton, MA):

$$I_{(t)} = A_1 \cdot e^{-(t-t_0)/\tau_1} + A_2 \cdot e^{-(t-t_0)/\tau_2} + I_\infty \quad (2)$$

with the following constraint:

$$A_1 + A_2 + I_\infty = 0 \quad \text{for } t = t_0 \quad \text{and } t_0 > 0 \quad (3)$$

In this formula, I_∞ is the stationary current for $t \rightarrow \infty$ and t_0 is a time offset which was introduced to account for a possible time lag due to the time-dependent release of ATP from caged ATP (a typical value for t_0 was 1 ms at pH 6.3). As data-analysis on the basis of Eq. 2 yields time constants τ_1 and τ_2 , the inverse of these values will be referred to as rate-constants k_1 and k_2 throughout the text.

As calculations based upon fitting results obtained on the basis of Eq. 2 led to an underestimation of the amount of transported charge per transport cycle (see Discussion), an alternative method of analysis was applied. This included a simple kinetic three-state model, based on a simplified Albers-Post-Scheme (Fahn et al., 1966, Post et al., 1969), which could be described by a system of differential equations containing a set of four independent parameters (k_1 , k_2 , k_3 , and Q ; see Appendix B). Although these equations can be solved analytically, a numerical least-squares algorithm was applied to fit the system of differential equations to the data using the program Scientist (MicroMath Scientific Software, Salt Lake City, UT). To speed up calculation, data traces were offline filtered at 500 Hz and reduced to 2-kHz sampling rate. Depending on the time course of a current signal, up to 500 data points (250 ms) were used for a single fit. The fitted results were virtually indistinguishable from those obtained by application of the model function from Eq. 2. As application of this method was very time consuming, only a selected set of data was analyzed in this way for the estimation of the turnover number of the Na^+/K^+ -ATPase.

Data analysis on the basis of the kinetic model from Appendix B was first developed and applied in a diploma thesis by T. Gropp (1995) at Max-Planck-Institut für Biophysik.

RESULTS

After obtaining a seal with a patch pipette (20- to $26\text{-}\mu\text{m}$ width) on the bleb from a ventricular myocyte, the patch was excised, continuously perfused with bath solution, and the patch current recorded. ATP was applied until a stable pump current was observed (see Fig. 2). By fast solution switches to different cytoplasmic solutions an ATP- and Na^+ -induced outward current was observed, as shown in Fig. 3 A, which reflects the transport activity of the sodium pump. The ATP dependence of this outward current is shown in Fig. 3 B; current values can be well fitted by a simple Michaelis-Menten type saturation function. The obtained K_m value of $\sim 150 \mu\text{M}$ is in good agreement with the K_m value for the low affinity ATP binding site (Post et al., 1972; Simons, 1974). In the absence of cytoplasmic Na^+ , ATP had no effect on the patch current (data not shown, see also Fig. 1 a in Nagel et al., 1992). The K_m value for Na^+ -activation of this Na^+ - and ATP-dependent outward current was determined to be $\sim 5 \text{ mM}$ Na^+ in the presence of $500 \mu\text{M}$ ATP (data not shown).

Inhibition of the Na^+ pump current by vanadate

Ortho-vanadate inhibits P-type ATPases in the micromolar concentration range (Cantley et al., 1977, 1978a,b; Beaugé and Glynn, 1978). To further prove that the ATP-induced outward current is solely related to the activity of Na^+/K^+ -ATPase, we studied the effect of switching to a vanadate-containing solution on the patch current. As can be seen in Fig. 4 A, the application of $100 \mu\text{M}$ ortho-vanadate leads to a rapid and complete inhibition of the ATP-induced outward current. Further experiments with different vanadate concentrations revealed, as expected, that the rate of this inhi-

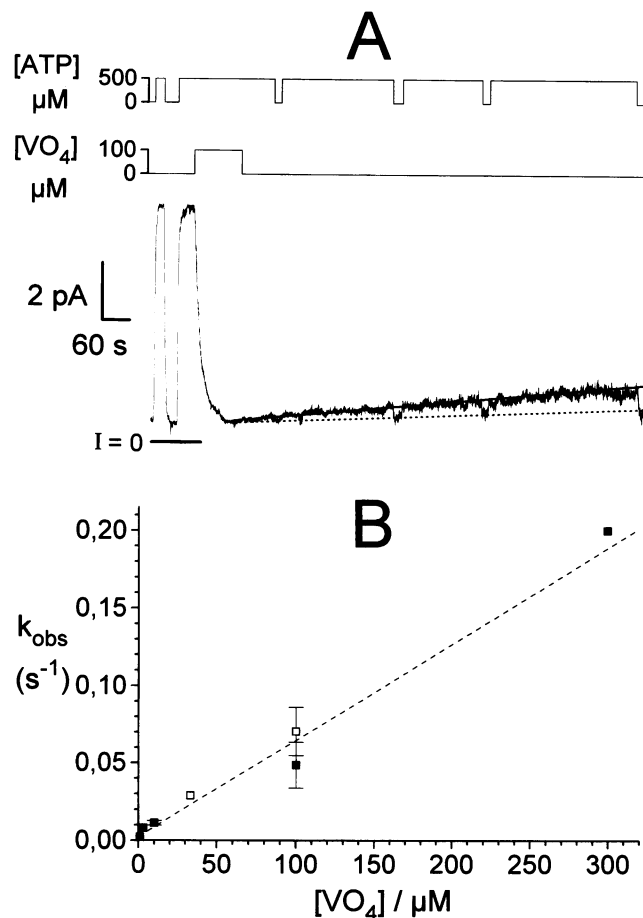


FIGURE 4 (A) Patch-current recording as response to superfusion with solutions containing 500 μM ATP, and inhibition with 100 μM orthovanadate, as indicated by the protocols in the upper section of A. Dissociation of vanadate in the presence of ATP shows slow recovery of the pump current with an estimated rate of 0.0003 s^{-1} (solid line). Pipette solution: P-Na-K, bath solution: B-F with MgATP added as indicated by protocol in the upper part, rat cell. (B) Dependence of the observed on-rates of inhibition by vanadate as a function of the vanadate concentration. Data were derived from a least-squares fit of a monoexponential decay function to the declining phase of the current recording, values are means \pm SD from several experiments. Pipette solution: P-Na-K (■) or P-NMG-K (□). Rat cells, $T = 24^\circ\text{C}$.

bition is dependent upon the concentration of vanadate; we obtained a value $k_{\text{on}} = 620 \text{ M}^{-1}\cdot\text{s}^{-1}$ (see Fig. 4 B). The inhibition by vanadate is reversible, although complete recovery of the pump activity in most cases cannot be obtained because of the very slow dissociation of vanadate, which exceeds the typical time range of a giant-patch experiment. k_{off} values were $\sim 3 \cdot 10^{-4} \text{ s}^{-1}$ in the absence of extracellular Na^+ ($n = 3$, see Fig. 4 A). Whereas Na^+ had no effect on the on-rate of the inhibition, recovery of the pump activity could be accelerated ~ 10 -fold, if 145 mM Na^+ was present on the extracellular side of the patch (data not shown). From the k_{on} and k_{off} values we can calculate an inhibition constant K_i of $\sim 0.5 \mu\text{M}$ ($[\text{Na}^+]_o = 0$).

Modulation of the Na^+ pump current by cytoplasmic pH

We were interested in the pH dependence of this ATP-induced outward-directed pump current, because this experimental approach easily allows the study of the influence of pH at the cytoplasmic side in contrast to whole cell experiments. Moreover, the kinetics of photolytic release of ATP from caged ATP is pH dependent (McCray et al., 1980) making it necessary to use low pH for high resolution kinetic measurements with caged ATP (Fendler et al., 1987, 1993). The extracellular pH (in the pipette) was held constant at 7.4. Fig. 5 A shows changes to solutions of different pH, followed by a solution change to an ATP-containing solution to measure the pump current at a given pH. A small reversible current shift can be observed upon decreasing pH,

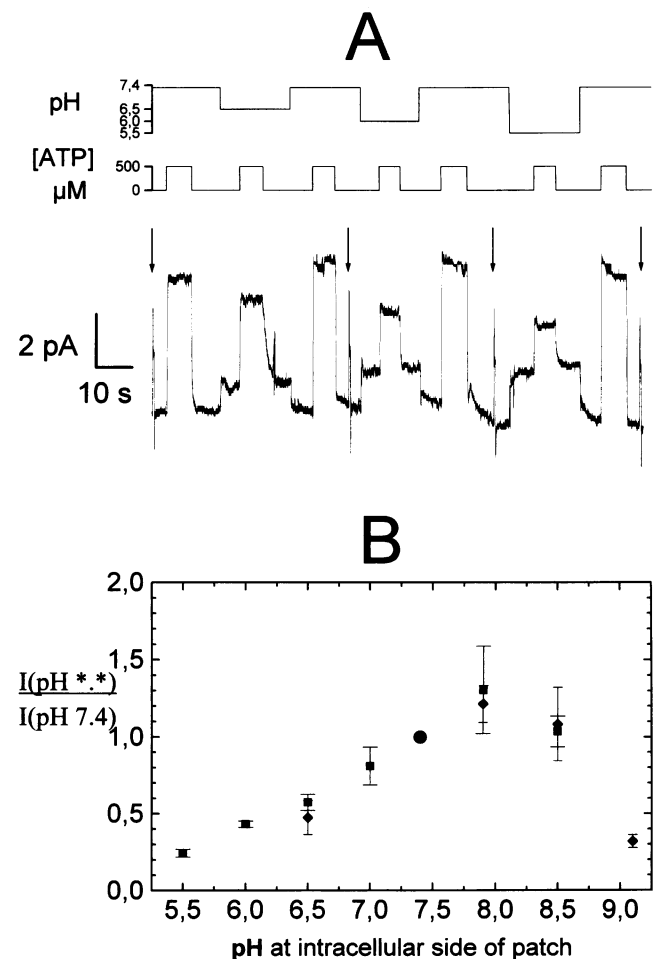


FIGURE 5 (A) Response of patch current to superfusion of the patch with solutions containing 500 μM ATP at different pH, as indicated by the schematic protocol in the upper part of the figure. Bath solution B-pH with or without 500 μM MgATP. Pipette solution: P-Na-K. Arrows indicate current response to a 10-mV pulse for the test of the seal resistance ($\approx 5 \text{ G}\Omega$). Rat cell, $T = 24^\circ\text{C}$. (B) Dependence of normalized patch current on internal pH, plotted are means \pm SD. (■) indicates rat, (◆) guinea pig cell experiments, values at pH 7.4 (●) were used to normalize currents. $T = 24^\circ\text{C}$.

the origin of which was not systematically investigated. Its magnitude was variable (probably depending on the seal resistance) and it is probably because of slight differences in osmolarity of the solutions. The ATP-induced pump current is clearly inhibited by lowering cytoplasmic pH, but this effect is completely reversible as can be seen at the end of the record in Fig. 5 A. A summary of the normalized ATP-induced pump currents at a pH range from 5.5 to 9.1 is shown in Fig. 5 B. It can be noted that the pump current at pH 6.3 still has about half the magnitude of the pump current at pH 7.4. Internal pH might affect the enzyme's affinities toward various substrates. Because our standard ATP concentration ($500 \mu\text{M}$) is the substrate concentration that is least saturating (about three times the $K_{1/2}$ for ATP), we measured the ATP dependence of the pump-current at pH 6.3, which indicated no significant change in the apparent ATP-affinity at that pH (data not shown).

Dependence of the pump current on temperature

As mentioned above, in different approaches to studying the kinetics of the transport steps in Na^+, K^+ -ATPase, different preparations as well as different temperatures were used. In this case, a comparison of the obtained rates is easier if the activation energy is known. Of course the activation energy for the overall transport cycle is not necessarily identical to the activation energy for a particular partial reaction, e.g., the Na^+ -translocation step. Fig. 6 A shows a record of the temperature in the measuring chamber together with a record of the patch current obtained in the presence of $500 \mu\text{M}$ ATP, but with brief changes to the ATP-free solution to account for temperature-dependent changes of the patch current. It can be seen that the patch current in the absence of ATP increases slightly with increasing temperature, but the ATP-activated current increases even more so. After estimation (by interpolation with an empirical formula) of the temperature dependence of the patch current in the absence of ATP, we subtracted it from the total current to get the temperature dependence of the ATP-activated pump current. We then plotted the logarithm of the ATP-activated current in an Arrhenius plot against the inverse of absolute temperature (see Fig. 6 B, results from seven different experiments) to calculate the activation energy for the pump current. The activation energy is quite high, ~ 92 kJ/mol (in the range of 22 to 30°C), and there is a change at $\sim 22^\circ\text{C}$ to an even higher activation energy of ~ 150 kJ/mol in the low temperature range (13– 21°C). The pH of the bath solution also changed slightly with temperature. Thus, we empirically determined the temperature dependence of the buffer's pH. With the given pH dependence of the pump current (as shown in Fig. 5 B), we calculated scaling factors to correct the pump current for the change of pH with temperature. This correction mainly affects the activation energy in the temperature range above 22°C and leads to a value of 100 kJ/mol (instead of 92 kJ/mol) between 22 and 30°C .

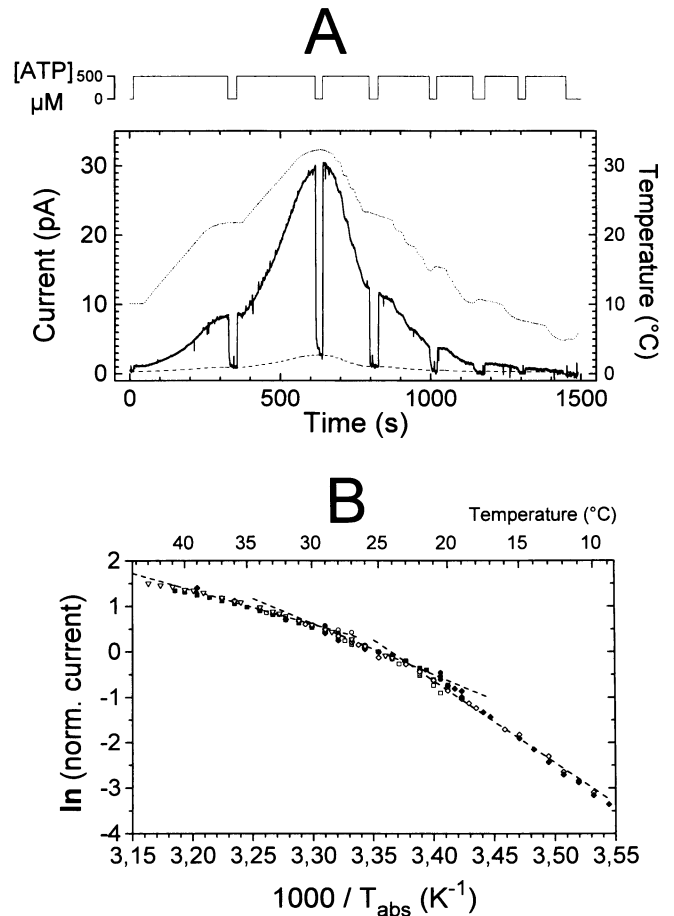


FIGURE 6 (A) Dependence of patch current on temperature: Temperature of the perfusion solution was varied as indicated by the temperature protocol (upper, dotted trace, referring to right scale), patch current is the middle, solid line (referring to left scale). Patch current recording including switches to a solution without ATP, to test variations of the baseline current with temperature. Baseline current was interpolated according to its exponential dependence on temperature between the switches to ATP free solution (lower, dashed line). Pump current was calculated as the difference between the recorded patch current and the interpolated baseline, guinea pig cell. (B) Arrhenius plot of seven pump current recordings from seven different guinea pig cells. Dashed lines refer to two different activation energy values for different temperature ranges (92 kJ/mol for $22^\circ\text{C} < T < 30^\circ\text{C}$, 150 kJ/mol for $13^\circ\text{C} < T < 22^\circ\text{C}$). Bath solution: B-F with or without $500 \mu\text{M}$ ATP as indicated in the upper section of (A). Pipette solution: P-NMG-K.

Inhibition of the pump current by caged ATP

The nonhydrolyzable (photocleavable) ATP-analog, caged ATP, binds to the Na^+, K^+ -ATPase and therefore acts as a competitive inhibitor (Forbush, 1984; Nagel et al., 1987; Fendler et al., 1993). We limited fast solution exchange experiments with caged ATP to the concentration range that we expected to be most relevant for photolysis experiments because of the relatively high consumption of solution during continuous perfusion. In a photolysis experiment, the fraction of caged ATP that is converted to ATP can be adjusted by the intensity of the irradiation. In solution exchange experiments, the pump current was activated by

100 μM ATP or mixtures of 100 μM ATP and increasing concentrations of caged ATP as shown in Fig. 7. It can be seen that at higher caged-ATP concentrations the pump current is inhibited. From these experiments and the assumption that caged ATP inhibits the pump current by competitive binding, we concluded that inhibition occurs at the high affinity ATP binding site K_{m1} with a ratio of K_I to K_{m1} of ~ 13 (see Discussion and fit curve in Fig. 7).

Fast activation of the pump current by photolytic release of ATP

Fig. 8 A shows the response of the patch current to an ATP concentration jump using photolysis of caged ATP at pH 7.4. Fig. 8 B demonstrates the inhibition of this signal by pretreatment of the same patch with ortho-vanadate. Because photolysis of caged ATP is catalyzed by H^+ and has a time constant of ~ 25 ms at pH 7.4 (McCray et al., 1980; Walker et al., 1988), the slow rise of the signal was attributed to this slow ATP release. Further experiments were done at pH 6.3, where photolytic release of ATP takes place in ~ 2 ms.

A typical laser flash photolysis experiment is shown in Fig. 9 at low time resolution. A pump current of ~ 15 pA could be activated by 500 μM ATP at pH 7.4 (A in Fig. 9) corresponding to ~ 8 pA at pH 6.3 (C in Fig. 9). Ten laser flashes in the presence of 250 μM caged ATP led to repeated current spikes with a rapidly decaying stationary current (1–10 in Fig. 9) as expected from the reduction of ATP concentration by consumption via hexokinase and glucose as well as by dilution via diffusion. A rundown of pump current by repeated photolysis can be observed (compare D to C in Fig. 9), which is, however, not affecting the fitted rate constants (see Materials and Methods). Fig. 10

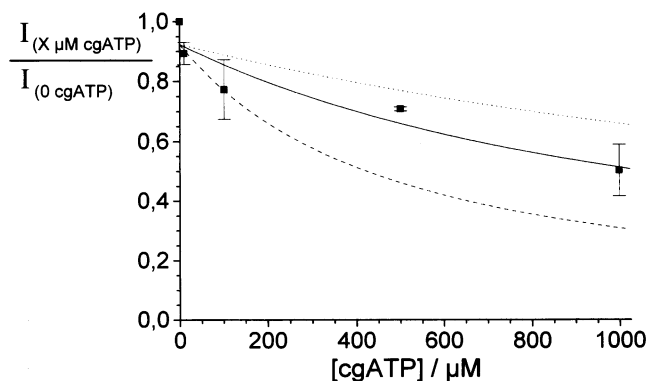


FIGURE 7 Dependence of patch current in the presence of 100 μM ATP on different concentrations of caged ATP added to the perfusion solution. The patch current was normalized to the current value in the presence of 100 μM ATP only, values are means \pm SE. Included are three simulations according to Eq. A5 in Appendix A, in which the mechanistic assumptions about the inhibition are described (solid line = best fit: $K_I/K_{m1} = 13$, dashed line: $K_I/K_{m1} = 5$, dotted line: $K_I/K_{m1} = 25$, see also Discussion). Bath solution: B-F plus 100 μM ATP. Pipette solution: P-NMG-K. Guinea pig cells, $T = 24^\circ\text{C}$.

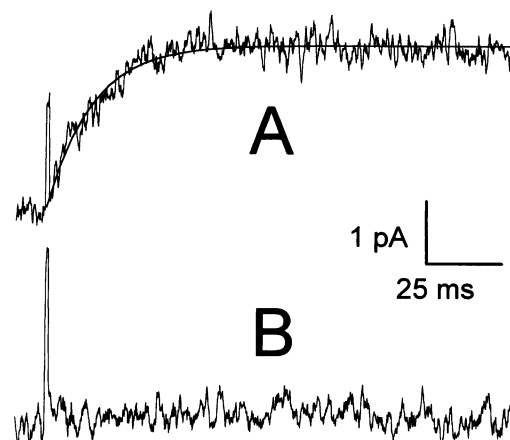


FIGURE 8 (A) Current signal in response to photolysis of 500 μM caged ATP with a release ratio of 30% at pH 7.4. After a short light-induced artifact a rise of the current to a stationary value can be observed, corresponding to the amount of released ATP. Included is a least-squares fit of a monoexponentially rising function to the data, leading to a rise time of 15 ms. (B) Current response to photolysis of 500 μM caged ATP on the same patch as in A, after inhibition of the stationary pump current by 1 mM ortho-vanadate. Bath solution: B-P. Pipette solution: P-NMG-K. Guinea pig cell, $T = 24^\circ\text{C}$.

shows the current responses at higher time resolution at three different flash intensities (resulting in three different concentrations of released ATP) from the same patch, to-

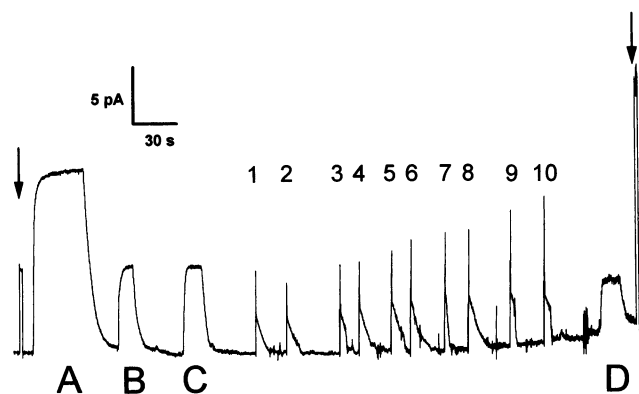


FIGURE 9 Low time resolution current recording of a typical photolysis experiment. A, B, C, and D indicate current responses to exchanges between solutions containing different amounts of ATP at two pH values: solution B-F + 500 μM ATP pH 7.4 (A); B-F + 100 μM ATP, pH 7.4 (B); B-F + 500 μM ATP, pH 6.3 (C and D). Between (C) and (D) is a series of laser flashes (Note rundown of stationary pump current after 10 flashes!). Numbers indicate UV flashes applied with different energy densities E (increasing order $E(1, 2) < E(3, 4) < E(5, 6) < E(7, 8) < E(9, 10)$) after injection of solution B-P, pH 6.3, containing 250 μM caged ATP. This leads to different amounts of released ATP, as can be seen from current amplitudes immediately after the light flash. As B-P solutions contain glucose and 10 units/ml hexokinase, pump currents decrease with a time constant of ~ 3 s, which can be seen in flashes 1, 2, 4, 5, 6, and 8. In signals 3, 9, and 10, new solution was injected several seconds after the flash, leading to a faster current decrease. Signal 7 was obtained by flashing during continuous inflow of caged-ATP solution. Photolysis signals of Fig. 10 are from this series. Pipette solution: P-NMG-K. Rat cell, $T = 24^\circ\text{C}$.

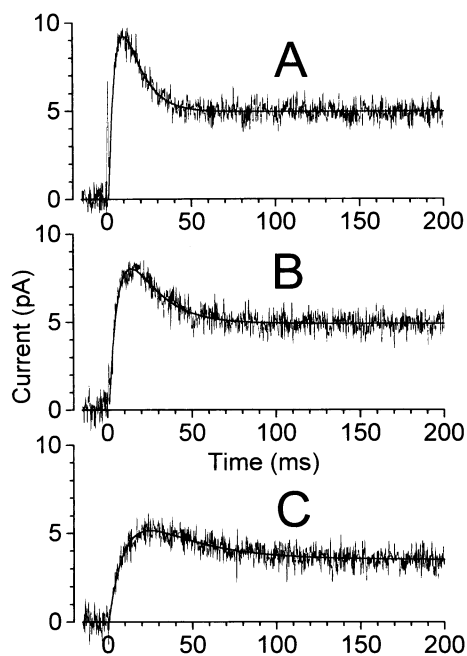


FIGURE 10 Current signals as a response to photolysis of 250 μM caged ATP at pH 6.3 in the same patch with different energies per u.v. light flash, leading to different concentrations of released ATP: (A) 61 μM , (B) 34 μM , (C) 12 μM . Included in the traces are least square fits to a function with a double exponential decay and a stationary component. A constraint was applied, forcing the fit function to start at zero current after a variable delay-time, which appeared to be around 1 ms. Bath solution: B-P with 250 μM caged ATP. Pipette solution: P-NMG-K. Rat cell, $T = 24^\circ\text{C}$.

gether with fit curves. In contrast to experiments at pH 7.4 (see Fig. 8), photolytic release of ATP at pH 6.3 resulted in a fast transient outward current, followed by a stationary outward current, which could be fitted by a sum of two exponential functions and a constant (see Eq. 2 in Materials and Methods). The problem of how to assign the obtained rate constants to certain steps in the Na^+, K^+ -ATPase transport cycle was solved by an analysis analogous to Fendler et al. (1987). The laser flash-induced signals were measured at different caged-ATP concentrations, but at a fixed conversion ratio (η), and the obtained rate constants k_1 and k_2 were plotted against the concentration of released ATP. Fig. 11 shows this dependence: an ATP-independent rate constant k_1 of $\sim 200 \text{ s}^{-1}$ and an ATP-saturable rate constant k_2 with a K_m for ATP of $\sim 6 \mu\text{M}$ (which varied with η , not shown).

A careful analysis of similar results, obtained with eel electroplax Na^+, K^+ -ATPase-containing vesicles adsorbed to a BLM, was undertaken by Fendler and co-workers (Fendler et al., 1993). This detailed study compared current measurements to measurements of phosphorylation and caged-ATP dissociation. As these data are not available for the heart cell Na^+, K^+ -ATPase, similarity can only be assumed. This would mean that k_2 reflects the sum of the nonelectrogenic steps, caged-ATP dissociation, and ATP binding, whereas k_1 reflects steps leading to the electrogenic Na^+ translocation, most likely phosphorylation and the E_1P to E_2P conformational change (see Discussion).

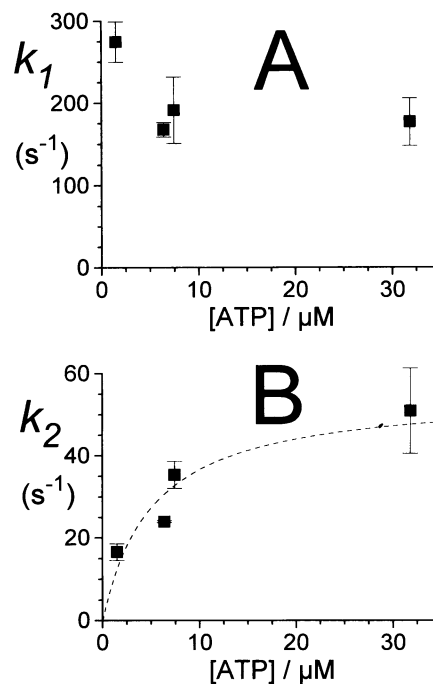


FIGURE 11 Dependence of rate constants k_1 (A) and k_2 (B) from photolytically-induced transient pump currents at pH 6.3 on the concentration of released ATP at a constant release ratio of 15%. A least square fit (dashed line) to a Michaelis-Menten equation is included in (B), leading to an apparent K_m of $5.1 \pm 2.5 \mu\text{M}$ and a V_{max} of $55 \pm 11 \text{ s}^{-1}$. Bath solution: B-P with 10 to 250 μM caged ATP. Pipette solution: P-NMG-K. Rat cells, $T = 24^\circ\text{C}$.

DISCUSSION

It was shown before that it is possible to study ion pumps under the well-defined conditions of an excised patch with the giant-patch technique (Hilgemann et al., 1991; Collins et al., 1992; Hilgemann, 1994). Here we applied, in addition, laser flash photolysis of caged ATP for a fast concentration jump of ATP.

Caged ATP was used to measure Na^+ efflux from vesicles in a single turnover of the Na^+, K^+ -ATPase (Forbush, 1984) or to measure transient currents from membrane fragments containing Na^+, K^+ -ATPase, which were capacitively coupled to a BLM (Fendler et al., 1985, 1987; Nagel et al., 1987; Borlinghaus et al., 1987). After characterization of the Na^+, K^+ -ATPase current in these excised patches by conventional solution exchange methods, we will compare the results obtained by flash photolysis of caged ATP to similar experiments undertaken before, especially with the BLM technique.

The ATP dependence of the Na^+, K^+ -ATPase

The ATP dependence of the pump current could be well fitted by a simple Michaelis-Menten saturation curve, see Fig. 3 A. The K_m for ATP is then $\sim 150 \mu\text{M}$ at 24°C in our experiments with rat or guinea pig myocytes, corresponding to the well-described low affinity ATP binding to E_2 , which

increases the rate of the E_2 to E_1 conformational change (Post et al., 1972) and therefore also the K_i^+/K_o^+ exchange (Simons, 1974). Although ATP binding to E_1 , preceding phosphorylation, has a K_m which is ~ 100 times smaller than that of the E_2 state (Glynn, 1985), this high affinity site was not readily detected under our conditions of saturating K_o^+ , presumably because of a very slow E_2 to E_1 conformational change at low ATP concentrations. This means α in Eq. A1 (see Appendix A) is much smaller than 1 and therefore Eq. A1 is reduced to a simple Michaelis-Menten saturation curve as in Eq. A3.

Inhibition of the Na^+ pump current by vanadate

Since Cantley et al. (1977) identified ortho-vanadate (VO_4^{3-}) as a potent inhibitor of Na^+, K^+ -ATPase, numerous experimental approaches have been undertaken to study the inhibitory effect of this anion on the enzyme (Cantley et al., 1978a,b; Smith et al., 1980). Here it was possible to measure the on- and the off-rate of inhibition (k_{on} , k_{off}) by ortho-vanadate by measuring the pump current after addition (and removal) of vanadate. The shape of the decay curves could be well described by a single exponential function for all vanadate concentrations tested (1–300 μM). As can be seen from Fig. 4 B, a linear relationship between vanadate concentration and the observed relaxation rate k_{obs} exists, which can be explained by the simple reaction model from Eq. 4 (see below). No significant differences in k_{obs} or k_{off} were found between rat and guinea pig enzyme. However, because of the slow recovery of pump current, it was difficult to observe k_{off} within the lifetime of a membrane patch (typically 20 min). Under the assumption of a simple bimolecular reaction between vanadate (I) and the Enzyme (E) according to the following equation (Cantley et al., 1978b):



and given that $[I] \gg [E]$, the following relationship between observable (k_{obs}) and intrinsic (k_{on} , k_{off}) relaxation constants can be derived:

$$k_{obs} = k_{on} \cdot [I] + k_{off} \quad (5)$$

Least-squares fit of the data from Fig. 4 B to Eq. 5 leads to $k_{on} = 620 M^{-1} s^{-1}$, whereas k_{off} cannot be obtained reliably from these data. The direct observation of k_{off} (see Fig. 3 A) yielded $(3 \pm 1) \cdot 10^{-4} s^{-1}$ in the absence of extracellular Na^+ , which results in an apparent dissociation constant K_d of 0.5 μM .

Cantley et al. (1978b) obtained apparent relaxation rate constants $k_{on} = 6.5 \cdot 10^4 M^{-1} s^{-1}$ for the binding and $k_{off} = 0.0033 s^{-1}$ for the dissociation reaction at 37°C, with a dissociation constant ($K_d = k_{off}/k_{on}$) of 51 nM. They measured relaxation of ATP hydrolysis during equilibration of purified Na^+/K^+ -ATPase from dog kidney with ortho-vanadate. Smith et al. (1980) reported a k_{off} value of $8.9 \cdot 10^{-5} s^{-1}$

(0.32 h^{-1}) at 25°C in an assay comparable to Cantley et al. (1978b) in which the rate of vanadate release from the enzyme was measured. The apparent rate constant k_{off} could be accelerated twofold by addition of K^+ (with $K_{1/2} = 0.5$ mM) and 50-fold by addition of Na^+ ($K_{1/2} = 250$ mM). K^+ was also present in our experiments (5 mM) at the extracellular side. Although extracellular Na^+ did not affect the on-rate of inhibition by vanadate, an accelerating effect of Na_o^+ on k_{off} could also be observed in our experiments, suggesting a 10-fold increase in presence of 145 mM Na_o^+ .

Modulation of the Na^+ pump current by cytoplasmic pH

Pump currents show a marked maximum at $pH_i = 7.9$ declining to both higher and lower pH_i values. Determination of the influence of external pH on the pump current was beyond the scope of this study, as this would require the use of outside-out patches or of pipette perfusion. A dependence of a subpopulation of pumps on pH_o was reported (Gao et al., 1995), although surprisingly no influence of internal pH (or more precisely, pipette pH) on pump activity was found in this whole-cell patch-clamp study.

Breitwieser et al. (1987) concluded from detailed investigations on internally dialyzed and superfused squid axons that external pH has no influence on the pump activity. They studied ouabain-sensitive Na^+ -efflux as well as ouabain-sensitive K^+ -influx, concluding that the activity of both processes shows a "bell-shaped" dependence on internal pH, with a clear maximum at pH 7.4. A similar pH dependence was found by Forbush and Klodos (1991). They concluded that different steps within the reaction cycle may appear rate-limiting in different pH ranges. Thus, the dependence of Na^+/K^+ -ATPase activity on pH may be described as limited by the rate of K^+ deocclusion at acidic pH, and by the rate of Na^+ translocation at alkaline pH values (Forbush and Klodos, 1991).

Temperature dependence of the pump current

From the Arrhenius plot in Fig. 6 B, which represents the temperature dependence of the Na^+/K^+ -ATPase pump current from seven different guinea pig cells, an activation energy (E_A) of ~ 110 kJ/mol can be derived if only the values at 12 and 37°C are compared, assuming a linear Arrhenius plot. In the temperature range 22 to 30°C the plot is linear with an activation energy of ~ 100 kJ/mol. These values are in good agreement with previous experimental observations, carried out on a variety of different enzyme preparations. Marcus et al. (1986) report values of 91 to 115 kJ/mol for transport mediated by Na^+/K^+ -ATPase from rabbit kidney outer medulla reconstituted in lipid vesicles. E_A of ATPase activity was measured by several groups: Post et al. (1965) studied isolated enzyme in membrane fragments from guinea pig kidney and reported a value of 71 kJ/mol for temperatures from 18 to 44°C; Kimelberg and

Papahadjopoulos (1974) worked on rabbit kidney enzyme incorporated into artificial lipid vesicles (E_A values, measured below/above the transition temperature T_c of the lipid: 46/96 kJ/mol, $T_c = 28.1^\circ\text{C}$ for microsomes, solubilized enzyme yielded values between 59/125 kJ/mol, $T_c = 20.2^\circ\text{C}$ and to 139/291 kJ/mol, $T_c = 31.4^\circ\text{C}$, depending on lipid used for solubilization); White and Blostein (1982) measured ATPase activity of enzyme from human red cells and guinea pig kidney outer cortex (activity was measured at 0 and 37°C , from the stated values one can calculate an E_A of ~ 90 kJ/mol for both enzyme sources); and Kaplan and Kenney (1985) investigated enzyme from red cells (from ATPase activity figures at 5 and 37°C an E_A value of 120 kJ/mol can be derived).

As can be seen from Fig. 6 B, a discontinuity in the slope of the Arrhenius plot appears at around 22°C and at $\sim 30^\circ\text{C}$, which could be observed in all experiments covering that temperature range. E_A appears to be ~ 150 kJ/mol below 22°C and only ~ 60 kJ/mol above 30°C . Esman and Skou (1988) report comparable values for the activation energy of Na^+/K^+ -ATPase activity in membrane fragments of ox kidney, ox brain, and shark rectal glands, with Arrhenius plots showing a smooth decrease in slope at higher temperatures. However, significance and interpretation of such changes in slope appear to be ambiguous and a variety of explanations have been suggested for each individual enzyme. One possibility is a change of the rate-limiting step. Partial reactions within an enzyme's reaction cycle may have different activation energies such that different steps appear rate-limiting in different temperature ranges.

A discontinuity also might occur, if the apparent affinity for one substrate shows such a strong temperature dependence that substrate saturation conditions may become violated. It seems improbable however, that cation affinities change to such an extent that apparent K_m values approach our experimental concentrations. In the absence of external Na^+ our K_o^+ concentration of 5 mM is ~ 20 times higher than the apparent K_m for K_o^+ (Nakao and Gadsby, 1989) and our internal Na^+ concentration is eight times higher than apparent K_m for Na^+ (our study and Collins et al., 1992). But, as outlined before, the concentration of ATP was only about three times higher than its K_m . The apparent K_m for ATP would have to rise with temperature. There are studies reporting such an effect in intact red blood cells (Marjanovic and Willis, 1992). This is not observed, however, with broken membrane preparations within the same study. In giant-patch studies carried out with guinea pig heart cells at 34 – 36°C , an apparent K_m for ATP of $94 \mu\text{M}$ (Collins et al., 1992) was found. This implies a slight increase in apparent affinity, which cannot account for the change in slope.

A considerable rundown of pump activity during the experiment could also result in a decrease of steepness of the Arrhenius plot. But, three experiments (out of seven in Fig. 6 B), in which it was possible to measure the pump current at the same temperature at the beginning and the end of an experiment, showed that the slight rundown of pump

current within the experimental time range could not explain the observed discontinuity.

The inhibition by caged ATP

When examining the Na^+,K^+ -ATPase reaction cycle, where ATP acts stimulating at a high affinity site (leading to phosphorylation of the enzyme) and also at a low affinity site (increasing the rate of the E_2 to E_1 conformational change), it is straightforward to postulate that the nonhydrolysable caged ATP inhibits at the high affinity site, which was also shown before in phosphorylation (Fendler et al., 1993) and electrical (Nagel et al., 1987; Fendler et al., 1993) measurements. Therefore, we applied a model with high and low affinity ATP binding and inhibition of caged ATP at the high affinity site (see Appendix A). Simplifying Eq. A4 by a reasonable approximation ($\alpha \ll 1$, for which we have evidence (see Fig. 3 B) and $c_{\text{ATP}} \gg K_{m1}$, which is certainly true with $c_{\text{ATP}} = 100 \mu\text{M}$ and $K_{m1} \approx 1 \mu\text{M}$) we obtain Eq. A5 and can fit the data of Fig. 7 with it. From this analysis we obtained a value of 13 for the ratio of K_1/K_{m1} (see fit in Fig. 7) and therefore a K_1 in the low micromolar range. The action of caged ATP at the low affinity site is not clear at the moment. It would probably best be investigated by testing its influence on the $\text{K}_i^+/\text{K}_o^+$ exchange, which is stimulated by some nonhydrolyzable ATP analogs (Simons, 1975).

Fast activation of the pump current by photolytic release of ATP at pH 7.4

A fast substrate concentration jump can reveal kinetic constants of the partial reactions of an enzymatic reaction cycle. Photolysis of a nonhydrolysable ATP precursor (caged ATP) was introduced as an elegant way for a fast concentration change without mechanical perturbation that is even possible inside closed membrane systems (Kaplan et al., 1978). Caged ATP meets several requirements for kinetic investigation of the Na^+,K^+ -ATPase: it cannot be hydrolyzed by the enzyme; it is stable for hours at room temperature if not exposed to UV light; and it can be efficiently converted to ATP by illumination with intense UV light. Some limitations, however, have to be considered: the rate of ATP release is pH- and Mg^{2+} -dependent (McCray et al., 1980; Walker et al., 1988) and caged ATP binds to the Na^+,K^+ -ATPase, therefore acting as a competitive inhibitor (Forbush, 1984; Nagel et al., 1987).

The first demonstration of the possibility of measuring fast partial reactions of the Na^+,K^+ -ATPase by photolysis of caged ATP was the measurement of Na^+ extrusion from vesicles containing Na^+,K^+ -ATPase with a rapid filtration technique (Forbush, 1984). The two reciprocal time constants describing the signal at 15°C were 14 and 6 s^{-1} , which are similar to the calculated values for release of ATP from caged ATP (18 s^{-1} ; Barabás and Keszthelyi, 1984; Walker et al., 1988) and the apparent rate constant of ATP

binding in the presence of caged ATP (5 s^{-1} ; see Fendler et al., 1993) under the conditions of the study of Forbush, 1984.

After it was shown in 1985 that an electrical current can be measured by activation of Na^+, K^+ -ATPase-containing membrane fragments adsorbed to a BLM via photolysis of caged ATP, two groups independently showed (Borlinghaus et al., 1987; Fendler et al., 1987) that kinetic information about Na^+ translocation by the Na^+, K^+ -ATPase can be obtained by this technique. The main difference between our measurements and the BLM experiments is that we use the DC-coupled measurement of current in contrast to the AC-coupled measurement via the capacitance of the BLM, thereby eliminating the problem of calculating the true pump current (Apell et al., 1987) or of taking into account the system time constant of the measuring circuit (Fendler et al., 1987, 1993). This means that in contrast to BLM measurements, we directly measure a stationary pump current, and we can also be absolutely certain that the membrane potential applied to the Na^+, K^+ -ATPase is tightly controlled and is independent of the pump activity.

At the physiological pH of 7.4 and 2 mM Mg^{2+} (conditions as in Fig. 8 A), release of ATP at 24°C proceeds with a rate of $\sim 40 \text{ s}^{-1}$ (Barabás and Keszthelyi, 1984; Walker et al., 1988). Correspondingly we found a single exponentially increasing pump current upon photolysis of caged ATP at pH 7.4 (Fig. 8 A). The rate of this increase was found to be 70 s^{-1} , but, as revealed by experiments under different conditions (data not shown), it is dependent upon caged-ATP concentration and light intensity, i.e., the conversion ratio of caged ATP to ATP. That the time constant for the rise of the pump current could be faster than the time constant for ATP release was to be expected. The activation of the enzyme is approximately rate-limited by the time needed for releasing a nearly saturating ATP concentration and not by the time constant of ATP release. Therefore, the jump to a saturating ATP concentration could be made very fast by a very high initial caged-ATP concentration. But this approach is limited by the inhibitory binding of caged ATP to the enzyme, which makes the on- and off-rate of caged ATP to and from the ATPase an important modulator of the speed of activation of the ATPase, next to the rate of photolysis (Fendler et al., 1993). We therefore concluded that photolysis at pH 7.4 cannot provide intrinsic rate constants of the Na^+, K^+ -ATPase transport cycle.

Fast activation of the pump current by photolytic release of ATP at pH 6.3

The rate of flash-induced ATP release from caged ATP is dependent upon the concentration of Mg^{2+} ions and upon pH (Walker et al., 1988), whereby magnesium ions slow down the reaction and hydrogen ions speed it up. We chose pH 6.3 because the stationary current, i.e., enzyme turnover, is still about half compared to pH 7.4, and ATP release at pH 6.3, 2 mM Mg^{2+} , and 24°C proceeds with a rate of

$\sim 500 \text{ s}^{-1}$ (Barabás and Keszthelyi, 1984; Walker et al., 1988). As can be seen in Fig. 11, we found that the fast rise of the pump current (with rate constant k_1) is independent of the ATP concentration, whereas the slower decay to a stationary current (rate constant k_2) is ATP-concentration dependent. From our analysis of the ATP dependence of the rates, we conclude that the step that is rate-limiting the electrogenic event proceeds with a rate of 200 s^{-1} at 24°C, which is in good agreement with earlier estimates from caged-ATP experiments at pH 6.2 (Fendler et al., 1987, 1993), voltage jump experiments in oocytes (Rakowski, 1993; Holmgren and Rakowski, 1994), and giant cardiac membrane patches (Hilgemann, 1994). The remaining question of the pH dependence of this step will be investigated in a forthcoming study (Friedrich and Nagel, manuscript in preparation; see also Friedrich and Nagel, 1996).

A rate of 200 s^{-1} was also found for the electrogenic Na^+ translocation in the forward direction in voltage jump experiments on whole cell voltage-clamped myocytes (Nakao and Gadsby, 1986), but at 36°C. This rate was only $\sim 40 \text{ s}^{-1}$ at 20°C (Gadsby et al., 1992). This rate might be so slow in whole cell experiments on cardiac cells in contrast to our study and to voltage clamp experiments on oocytes from *Xenopus laevis* (Rakowski, 1993) because of some specific cardiac cellular regulation. Consistent with this explanation, a study of giant excised membrane patches from cardiac cells gave a rate of 600 s^{-1} at 36°C (Hilgemann, 1994), which, taking into account the activation energy, corresponds to a rate of $\sim 200 \text{ s}^{-1}$ at 24°C. Additional evidence for some not yet understood cellular down-regulation of the Na^+, K^+ -ATPase in cardiac cells comes from the observation that the pump current in excised giant patches slowly increases upon first application of ATP (see Fig. 2 and Hilgemann (1995b)), suggesting a higher turnover rate for the Na^+, K^+ -ATPase in excised patches compared to whole cell measurements.

Apell et al. (1987) (see also Wuddel and Apell (1995)) took the results from cardiac whole cell measurements (Nakao and Gadsby, 1986) as support for their conclusion from caged-ATP/BLM experiments (Borlinghaus et al., 1987) of a much slower electrogenic step: 25 s^{-1} at 20°C (e.g., Wuddel and Apell, 1995). But as pointed out above, the assignment of the observed rates to either ATP release or intrinsic ATPase reaction rates can be misleading if conditions are chosen (pH 7.2, 10 mM Mg, 20°C; Wuddel and Apell, 1995) where ATP release proceeds with a rate of only $\sim 40 \text{ s}^{-1}$ (Walker et al., 1988). The assignment of observed-rate constants to partial reactions can be supported by the variation of substrate concentration, which exhibited an ATP dependency of the decay rate k_2 in BLM experiments (Fendler et al., 1987) as well as in our experiments. This substrate dependence makes k_2 therefore a very unlikely candidate for an intrinsic Na^+, K^+ -ATPase rate constant in contrast to k_1 which is independent of the ATP concentration.

Comparing data from phosphorylation and BLM electrical measurements (Fendler et al., 1993) with voltage clamp

(Nakao and Gadsby, 1986; Rakowski, 1993; Holmgren and Rakowski, 1994) and giant-patch clamp experiments (Hilgemann, 1994), it seems most likely that phosphorylation of heart cell Na^+, K^+ -ATPase is fast and that the electrogenic $\text{E}_1\text{P}-\text{E}_2\text{P}$ conformational change proceeds with a rate constant of 200 s^{-1} at 24°C in excised membrane patches. This conclusion is not contradictory to an electro-neutral $\text{E}_1\text{P}-\text{E}_2\text{P}$ conformational change (with a rate constant of 200 s^{-1}) followed by a fast electrogenic Na^+ release (Hilgemann, 1994; Wagg et al., 1996), as put forward by access channel models for the Na^+, K^+ -ATPase (Gadsby et al., 1993; Hilgemann, 1994). In our experiments this mechanism would yield the same results because it is kinetically equivalent to an electrogenic $\text{E}_1\text{P}-\text{E}_2\text{P}$ conformational change.

Estimation of turnover rates

As shown in Fig. 10, fast activation of the Na^+, K^+ -ATPase molecules leads to a rapidly rising transient current followed by a constant steady-state current. This characteristic shape is most obvious at high ratios of ATP to caged ATP, as in Fig. 10 A. It is tempting to calculate the charge under the transient current component and to derive from it the number of pump molecules under the assumption that one unit charge is transferred per pump molecule. In the example of Fig. 10 A this leads to 80 fC, corresponding to $0.5 \cdot 10^6$ pump molecules. But because the steady-state current is not negligible this is a clear underestimation. Another approach is shown in Fig. 12 A where the signal was fitted numerically by a simple three-state model according to Appendix B. We obtained the following rate constants (according to the three-state model): $k_1 = 48 \text{ s}^{-1}$, $k_2 = 241 \text{ s}^{-1}$, and $k_3 = 30 \text{ s}^{-1}$. The scaling factor Q in this model is equivalent to the charge obtained if the number of pump molecules is multiplied with one unit charge. We obtained 270 fC, which brings the number of active pump molecules in the patch to $1.7 \cdot 10^6$. This charge is represented by the broken line in Fig. 12 A, obtained by the simulation of a single, but complete Na^+ translocation ($Q = 270 \text{ fC}$, $k_1 = 48 \text{ s}^{-1}$, $k_2 = 241 \text{ s}^{-1}$, and $k_3 = 0$). A turnover rate can then be calculated, either by the quotient of the steady-state current and the scaling factor Q or by the product of the steady-state concentration of one of the intermediates and its corresponding rate constant. The obtained steady-state turnover rate in the fit to Fig. 12 A is $\sim 17 \text{ s}^{-1}$ under these conditions. Fig. 12 B summarizes steady-state turnover rates from several patches at different ATP concentrations obtained by this fit procedure. It is obvious that the signal-to-noise ratio of our data allows for considerable scattering of the fit parameters. Nevertheless, a Michaelis-Menten fit to this ATP dependence resulted in a maximal turnover rate of 30 s^{-1} and a K_m for ATP of $43 \mu\text{M}$, which seems reasonable if compared to $150 \mu\text{M}$ from solution switch experiments (Fig. 3). It should be kept in mind that this ATP dependence is measured at a constant ratio of inhibitor

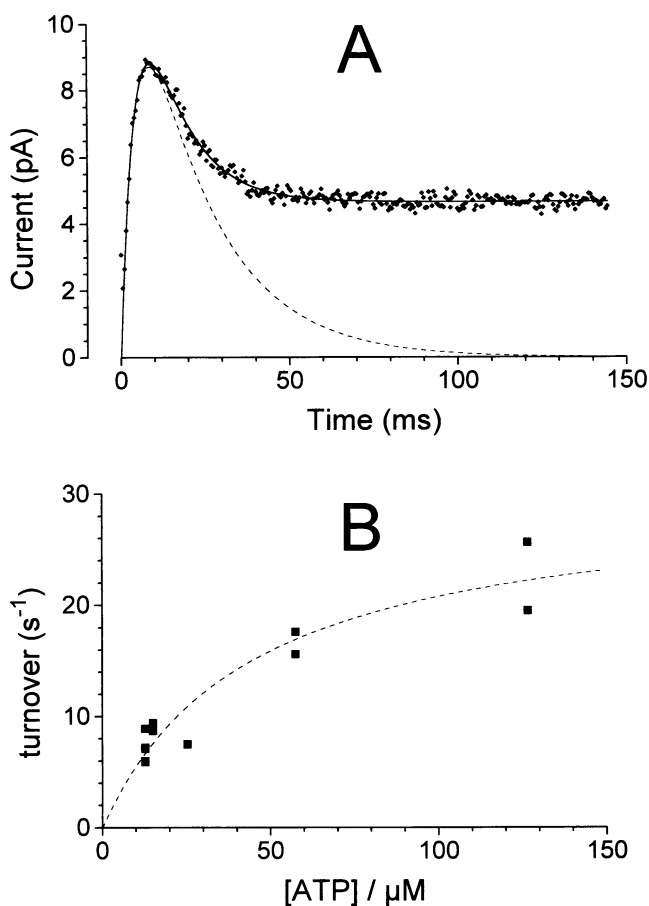


FIGURE 12 (A) Simulation of the data of Fig. 10 A with a simple three-state model yields estimates for the amount of transferred charge (number of pump molecules) and of the turnover rate. The constants obtained from the numerical fit are: scaling factor $Q = 270 \text{ fC}$, $k_1 = 48 \text{ s}^{-1}$, $k_2 = 241 \text{ s}^{-1}$, and $k_3 = 30 \text{ s}^{-1}$ resulting in a turnover rate of 17.2 s^{-1} . The amount of pump molecules transferring one unit charge per cycle, 270 fC, as obtained by the numerical fit, is represented by the dashed curve obtained by setting k_3 to 0. (B) ATP dependence of the fitted turnover rate at 24°C and pH 6.3 and at a constant ratio of ATP to caged ATP of 0.33. Included is a fit to a Michaelis-Menten type saturation with a K_m of $43 \mu\text{M}$ ATP and a maximal turnover of 30 s^{-1} . Pipette solution: P-NMG-K. Rat cells, $T = 24^\circ\text{C}$.

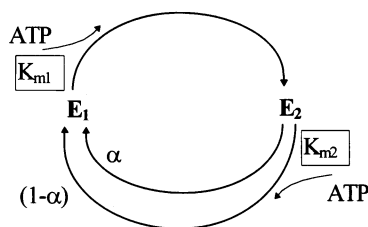
(caged ATP) to substrate (ATP), which tends to decrease the apparent K_m (Nagel et al., 1987). The scaling factor Q has to be different with different patches but it should remain the same or slightly decrease within each flash at the same patch because of the gradual photolysis-induced rundown of the pump current, as shown in Fig. 9. This was indeed observed, e.g., the value of Q obtained from the numerical fit to the signal at the beginning of the experiment (flash 1 in Fig. 9 = Fig. 10 C) was 500 fC and decreased to 270 fC later on (flash 9 in Fig. 9 = Fig. 10 A). The obtained turnover rate of 30 s^{-1} for saturating ATP concentrations at 24°C and pH 6.3 can now be converted (taking the pH dependence of Fig. 5 B) to get the turnover rate at pH 7.4 and 24°C , yielding 60 s^{-1} . With the help of our temperature dependence (Fig. 6 B) we can also get a turnover rate at

36°C and pH 7.4, resulting in 200 s^{-1} . This maximal turnover rate is slightly higher than that of partially purified Na^+, K^+ -ATPase from pig kidney ($\sim 170 \text{ s}^{-1}$ at 37°C; Jørgensen, 1980) but more than twice that reported for whole-cell patch clamp measurements on guinea pig myocytes (81 s^{-1} at 36°C; Gadsby and Nakao, 1989). This discrepancy in maximal turnover rates derived from pump current measurements on heart cell plasma membranes resembles the discrepancy that was found for the rate-limiting step in the Na^+ translocation pathway. Again, it might be explained if the turnover of the Na^+, K^+ -ATPase is down-regulated when measured in intact heart cells (as discussed above and suggested by Fig. 2). Further experiments should also include measurement of the membrane patch capacitance to provide additional information about the density of Na^+, K^+ -ATPase molecules in the membrane.

This new method to measure partial reactions of the Na^+, K^+ -ATPase should provide a useful tool for further elucidation of rate constants of wild type and mutated pump molecules especially as it is also well suited for giant patches from *Xenopus* oocytes (Niu et al., 1996). With suitable caged substrates the method can also be applied to other electrogenic transporters, as shown (with caged Ca^{2+}) for the $\text{Na}^+ - \text{Ca}^{2+}$ exchanger from cardiac plasma membrane (Kappl and Hartung, 1996).

APPENDIX A

A kinetic two-state model for the interaction of ATP with the two conformational states of the Na^+/K^+ -ATPase (E_1, E_2) is shown in Scheme 1. ATP is bound to E_1 with high affinity K_{m1} . Furthermore, ATP can stim-



Scheme 1

ulate the E_2 to E_1 conformational change by acting on a binding site with low affinity K_{m2} . α was introduced to allow for the fact that the rate of the E_2 to E_1 conformational change is not zero under zero ATP conditions, but under our conditions $\alpha \ll 1$. Under the kinetic and mechanistic assumptions given in the above model, which take into account that ATP can act both at a high and a low affinity binding-site, the influence of ATP (concentration = c_{ATP}) on the total turnover (V) of the Na^+, K^+ -ATPase can be described by the following equation (see also Reynolds et al., 1985):

$$V = \frac{\alpha \cdot V_{\text{max}} \cdot c_{\text{ATP}}}{K_{m1} + c_{\text{ATP}}} + \frac{(1 - \alpha) \cdot V_{\text{max}} \cdot c_{\text{ATP}}^2}{(K_{m1} + c_{\text{ATP}}) \cdot (K_{m2} + c_{\text{ATP}})} \quad (\text{A1})$$

Given, that $\alpha \ll 1$ leads to:

$$V \approx \frac{V_{\text{max}} \cdot c_{\text{ATP}}^2}{(K_{m1} + c_{\text{ATP}}) \cdot (K_{m2} + c_{\text{ATP}})} \quad (\text{A2})$$

and with $c_{\text{ATP}} \gg K_{m1}$ follows:

$$V \approx \frac{V_{\text{max}} \cdot c_{\text{ATP}}}{K_{m2} + c_{\text{ATP}}} \quad (\text{A3})$$

Thus, under the assumptions $\alpha \ll 1$ and $K_{m1} \gg c_{\text{ATP}}$ the complex relationship between V and c_{ATP} transforms into an equation of Michaelis-Menten type with a single binding site.

Because the inhibitory effect of caged ATP on the rate of Na^+, K^+ -ATPase phosphorylation is established (Fendler et al., 1993), we assume that caged ATP (concentration = c_i) acts as a competitive inhibitor (with inhibitor constant K_i) at the high affinity ATP binding site K_{m1} , disregarding its possible (but so far unknown) action at the low affinity site. Thus, we can express the turnover in the presence of ATP and caged ATP as follows:

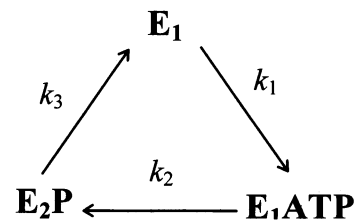
$$V = \frac{\alpha \cdot V_{\text{max}} \cdot c_{\text{ATP}}}{(1 + c_i/K_i) \cdot K_{m1} + c_{\text{ATP}}} + \frac{(1 - \alpha) \cdot V_{\text{max}} \cdot c_{\text{ATP}}^2}{(K_{m1} + K_{m1} \cdot c_i/K_i + c_{\text{ATP}}) \cdot (K_{m2} + c_{\text{ATP}})} \quad (\text{A4})$$

Again, if $\alpha \ll 1$ and $c_{\text{ATP}} \gg K_{m1}$:

$$V \approx \frac{V_{\text{max}} \cdot c_{\text{ATP}}^2}{((K_{m1} \cdot c_i/K_i) + c_{\text{ATP}}) \cdot (K_{m2} + c_{\text{ATP}})} \quad (\text{A5})$$

APPENDIX B

Current signals can be analyzed on the basis of a kinetic model representing a simplified Albers-Post-Scheme (Fahn et al., 1966; Post et al., 1969), as put forward by Fendler et al. (1993):



Scheme 2

The following considerations and assumptions apply:

1) As the forward rate constants are much faster than the backward rate constants (concentrations of ADP, P_i , Na_o^+ , and K_i^+ are zero), all steps are assumed to be irreversible.

2) The binding and exchange of ATP/caged ATP according to the reaction sequence $E_1 \text{ caged ATP} \leftrightarrow E_1 \rightarrow E_1 \text{ ATP}$ can be summarized in a single step $E_1 \rightarrow E_1 \text{ ATP}$ with an effective rate constant k_1 as described by Fendler et al., 1993.

3) There is only a single electrogenic step coinciding with the translocation of a single charge during the $E_1 \text{ P} \rightarrow E_2 \text{ P}$ conformational transition. Notably, this interpretation is kinetically equivalent to an electroneutral conformational change followed by an electrogenic Na^+ -binding/deocclusion process, as put forward in access channel models for the Na^+, K^+ -ATPase (Gadsby et al., 1993; Hilgemann, 1994). In contrast to the work of Fendler et al. (1993) phosphorylation cannot be resolved as an independent process in our experiments. Thus, phosphorylation and the electrogenic event ($E_1 \text{ ATPNa}^+ \rightarrow E_1 \text{ PNa}^+ \rightarrow E_2 \text{ P} + \text{Na}^+$) are included in a single step with an effective rate constant k_2 .

4) All reactions after the electrogenic step are included in the last transition $E_2 \text{ P} \rightarrow E_1$, which proceeds with the rate constant k_3 .

The differential equations describing this kinetic model are as follows:

$$\frac{d[E_1]}{dt} = k_3 \cdot [E_2P] - k_1 \cdot [E_1]$$

$$\frac{d[E_1ATP]}{dt} = k_1 \cdot [E_1] - k_2 \cdot [E_1ATP]$$

$$\frac{d[E_2P]}{dt} = k_2 \cdot [E_1ATP] - k_3 \cdot [E_2P]$$

The initial conditions are: $[E_1]_{(t=0)} = 1$; all others are 0.

With $(d/dt)([E_1] + [E_1ATP] + [E_2P]) = 0$, it follows that $([E_1] + [E_1ATP] + [E_2P])$ for all times t . The pump current is proportional to the time-dependent concentration of the intermediate E_1ATP :

$$I_p(t) = Q \cdot k_2 \cdot [E_1ATP](t)$$

The kinetic model described above contains four independent parameters: k_1 , k_2 , k_3 , and Q . Although the system of differential equations can be solved analytically, these solutions will not be described in detail and numerical analysis of the data was performed by fitting the system of differential equations to the data. Q is a scaling factor, which is used to adjust the amplitude of the current $I_p(t)$ and represents the amount of charge, which is translocated during one complete reaction cycle of the whole ensemble of enzyme molecules within the membrane patch.

We thank Drs. K. Fendler, J. Froehlich, and R. Clarke for fruitful discussions and careful reading of the manuscript; M. Kappl for improvements in our common setup; T. Gropp for help with the numerical fitting; and Mrs. D. Ollig and D. Stiebert for excellent technical assistance.

This work was supported by the Max-Planck-Gesellschaft and the Deutsche Forschungsgemeinschaft (SFB169).

REFERENCES

- Apell, H.-J., R. Borlinghaus, and P. Läuger. 1987. Fast charge translocations associated with partial reactions of the Na, K, pump. II. Microscopic analysis of transient currents. *J. Membr. Biol.* 97:179–191.
- Barabás, K., and L. Keszthelyi. 1984. Temperature dependence of ATP release from "caged" ATP. *Acta Biochim. Biophys. Acad. Sci. Hung.* 19:306–309.
- Beaugé, L. A., and I. M. Glynn. 1978. Commercial ATP containing traces of vanadate alters the response of $(Na^+ + K^+)$ -ATPase to external potassium. *Nature.* 272:551–552.
- Borlinghaus, R., H.-J. Apell, and P. Läuger. 1987. Fast charge translocations associated with partial reactions of the Na, K-pump. I. Current and voltage transients after photochemical release of ATP. *J. Membr. Biol.* 97:161–178.
- Breitwieser, G. E., A. A. Altamirano, and J. M. Russell. 1987. Effects of pH changes on sodium pump fluxes in squid giant axon. *Am. J. Physiol.* 253:C547–C554.
- Cantley, L. C., Jr., L. G. Cantley, and L. Josephson. 1978b. A characterization of vanadate interactions with the (Na, K) -ATPase. Mechanistic and regulatory implications. *J. Biol. Chem.* 253:7361–7368.
- Cantley, L. C., Jr., L. Josephson, R. Warner, M. Yanagisawa, C. Lechene, and G. Guidotti. 1977. Vanadate is a potent (Na, K) -ATPase inhibitor found in ATP derived from muscle. *J. Biol. Chem.* 252:7421–7423.
- Cantley, L. C., Jr., M. Resh, and G. Guidotti. 1978a. Vanadate inhibits the red cell (Na, K) -ATPase from the cytoplasmic side. *Nature.* 272:552–554.
- Collins, A., A. V. Somlyo, and D. W. Hilgemann. 1992. The giant cardiac membrane patch method: Stimulation of outward Na^+ - Ca^{2+} exchange current by MgATP. *J. Physiol.* 454:27–57.
- Esman, M., and J. C. Skou. 1988. Temperature-dependencies of various catalytic activities of membrane-bound Na^+/K^+ -ATPase from ox brain, ox kidney and shark rectal gland and of $C_{12}E_8$ -solubilized shark Na^+/K^+ -ATPase. *Biochim. Biophys. Acta.* 944:344–350.
- Fahn, S., G. J. Koval, and R. W. Albers. 1966. Sodium-potassium-activated adenosine tri-phosphatase of *electrophorus* electric organ. *J. Biol. Chem.* 241:1882–1889.
- Fendler, K., E. Grell, and E. Bamberg. 1987. Kinetics of pump currents generated by the Na^+, K^+ -ATPase. *FEBS Lett.* 224:83–88.
- Fendler, K., E. Grell, M. Haubs, and E. Bamberg. 1985. Pump-currents generated by the purified Na^+, K^+ -ATPase from kidney on black lipid membranes. *EMBO J.* 4:3079–3085.
- Fendler, K., S. Jaruschewski, A. Hobbs, W. Albers, and J. P. Froehlich. 1993. Pre-steady-state charge translocation in NaK-ATPase from eel electric organ. *J. Gen. Physiol.* 102:631–666.
- Forbush, B., III. 1984. Na^+ movement in a single turnover of the Na pump. *Proc. Natl. Acad. Sci. USA.* 81:5310–5314.
- Forbush, B., III, and I. Klodos. 1991. Rate-limiting steps in Na Translocation by the Na/K Pump. In *The Sodium Pump: Structure, Mechanism, and Regulation*. J. H. Kaplan and P. De Weer, editors. Rockefeller University Press, New York. 211–225.
- Friedrich, T., and G. Nagel. 1995. Transient and stationary Na^+, K^+ -ATPase currents in excised patches from rat heart cells induced by an ATP concentration jump. *Biophys. J.* 68:A256 [Abstract].
- Friedrich, T., and G. Nagel. 1996. Comparison of transient Na^+, K^+ -ATPase currents in excised patches from guinea pig heart cells induced by an ATP concentration jump or a voltage pulse. *Biophys. J.* 70:A18 [Abstract].
- Gadsby, D. C., and M. Nakao. 1989. Steady-state current-voltage relationship of the Na/K pump in guinea pig ventricular myocytes. *J. Gen. Physiol.* 94:511–537.
- Gadsby, D. C., M. Nakao, A. Bahinski, G. Nagel, and M. Suenson. 1992. Charge movements via the cardiac Na, K-ATPase. *Acta Physiol. Scand.* 146:111–123.
- Gadsby, D. C., R. F. Rakowski, and P. De Weer. 1993. Extracellular access to the Na/K-pump: pathway similar to ion channel. *Science.* 260:100–103.
- Gao, J., R. T. Mathias, I. S. Cohen, and G. J. Baldo. 1995. Two functionally different Na/K pumps in cardiac ventricular myocytes. *J. Gen. Physiol.* 106:995–1030.
- Glynn, I. M. 1985. The Na^+, K^+ -transporting adenosine triphosphatase. In *The Enzymes of Biological Membranes*, Vol. 3, 2nd ed. A. N. Martinosi, editor. Plenum Press, New York and London. 35–114.
- Glynn, I. M. 1993. All hands to the sodium pump (Annual review price lecture). *J. Physiol.* 462:1–30.
- Gropp, T. 1995. Ladungstransport durch die in Liposomen rekonstituierte NaK-ATPase. Diploma thesis. Universität Karlsruhe, Germany. 100 pp.
- Hilgemann, D. W. 1989. Giant excised cardiac sarcolemmal membrane patches: sodium and sodium-calcium exchange currents. *Pflügers Arch. Eur. J. Physiol.* 415:247–249.
- Hilgemann, D. W. 1994. Channel-like function of the Na, K pump probed at microsecond resolution in giant membrane patches. *Science.* 263:1429–1432.
- Hilgemann, D. W. 1995a. The Giant Membrane Patch. In *Single-Channel Recording*. B. Sakmann and E. Neher, editors. Plenum Press, New York. 307–327.
- Hilgemann, D. W. 1995b. Slow activation of Na/K pump on first application of ATP in giant patches: comparison to Na/Ca exchange. *Biophys. J.* 68: A307 [Abstract].
- Hilgemann, D. W., G. A. Nagel, and D. C. Gadsby. 1991. Na/K pump current in giant membrane patches excised from ventricular myocytes. In *The Sodium Pump: Recent Developments*. J. H. Kaplan and P. DeWeer, editors. The Rockefeller University Press, New York. 543–547.
- Holmgren, M., and R. F. Rakowski. 1994. Pre-steady-state transient currents mediated by the Na/K pump in internally perfused *Xenopus* oocytes. *Biophys. J.* 66:912–922.
- Isenberg, G., and U. Klöckner. 1982. Calcium tolerant ventricular myocytes prepared by preincubation in "KB medium". *Pflügers Arch.* 395:6–18.
- Jørgensen, P. L. 1980. Sodium and potassium ion pump in kidney tubules. *Physiol. Rev.* 60:864–917.

- Kaplan, J. H., and L. J. Kenney. 1985. Temperature effects on sodium pump phosphoenzyme distribution in human red blood cells. *J. Gen. Physiol.* 85:123-136.
- Kaplan, J. H., B. Forbush, III., and J. F. Hoffman. 1978. Rapid photolytic release of adenosine 5'-triphosphate from a protected analogue: utilization by the Na:K pump of human red blood cell ghosts. *Biochemistry.* 17:1929-1935.
- Kappl, M., and K. Hartung. 1996. Rapid charge translocation by the cardiac $\text{Na}^+\text{-Ca}^{2+}$ exchanger after a Ca^{2+} concentration jump. *Biophys. J.* 71: This issue.
- Kimelberg, H. K., and D. Papahadjopoulos. 1974. Effects of phospholipid acyl chain fluidity, phase transitions, and cholesterol on $(\text{Na}^+ + \text{K}^+)\text{-stimulated}$ adenosine triphosphatase. *J. Biol. Chem.* 249:1071-1080.
- Läuger, P. 1991. Na, K-ATPase. In *Electrogenic Ion Pumps*. Sinauer Associates Inc., Sunderland, UK. 168-306.
- Lingrel, J. B. 1992. Na, K-ATPase: isoform structure, function, and expression. *J. Bioeng. Biomembr.* 24:263-270.
- Marcus, M. M., H.-J. Apell, M. Roudna, R. A. Schwedener, H.-G. Weder, and P. Läuger. 1986. $(\text{Na}^+ + \text{K}^+)\text{-ATPase}$ in artificial lipid vesicles: influence of lipid structure on pumping rate. *Biochim. Biophys. Acta.* 854:270-278.
- Marjanovic, M., and J. S. Willis. 1992. ATP dependence of $\text{Na}^+\text{-K}^+$ pump of cold-sensitive and cold-tolerant mammalian red blood cells. *J. Physiol.* 456:575-590.
- McCray, J. A., L. Herbet, T. Kihara, and D. R. Trentham. 1980. A new approach to time-resolved studies of ATP-requiring biological systems: laser flash photolysis of caged ATP. *Proc. Natl. Acad. Sci. USA.* 77: 7237-7241
- Nagel, G., K. Fendler, E. Grell, and E. Bamberg. 1987. Na^+ currents generated by the purified $(\text{Na}^+ + \text{K}^+)\text{-ATPase}$ on planar lipid membranes. *Biochim. Biophys. Acta.* 901:239-249
- Nagel, G., T.-C. Hwang, K. L. Nastiuk, A. C. Nairn, and D. C. Gadsby. 1992. The protein kinase A-regulated cardiac Cl^- channel resembles the cystic fibrosis transmembrane conductance regulator. *Nature.* 360:81-84.
- Nakao, M., and D. C. Gadsby. 1986. Voltage dependence of Na translocation by the Na/K pump. *Nature.* 323:628-630.
- Nakao, M., and D. C. Gadsby. 1989. [Na] and [K] dependence of the Na/K pump current-voltage relationship in guinea pig ventricular myocytes. *J. Gen. Physiol.* 94:539-565.
- Niu, L., R. W. Vazquez, G. Nagel, T. Friedrich, E. Bamberg, R. E. Oswald, and G. P. Hess. 1996. Rapid chemical kinetic techniques for investigations of neurotransmitter receptors expressed in *Xenopus* oocytes. *Proc. Natl. Acad. Sci. USA.* 93: In press.
- Post, R. L., C. Hegyvary, and S. Kume. 1972. Activation by adenosine triphosphate in the phosphorylation kinetics of sodium and potassium transporting adenosine triphosphatase. *J. Biol. Chem.* 247:6530-6540.
- Post, R. L., S. Kume, T. Tobin, B. Orcutt, and A. K. Sen. 1969. Flexibility of an active center in sodium-plus-potassium adenosine triphosphatase. *J. Gen. Physiol.* 54:306s-326s.
- Post, R. L., A. K. Sen, and A. S. Rosenthal. 1965. A phosphorylated intermediate in adenosine triphosphatase-dependent sodium and potassium transport across kidney membranes. *J. Biol. Chem.* 240:1437-1444
- Rakowski, R. F. 1993. Charge movements by the Na/K pump in *Xenopus* oocytes. *J. Gen. Physiol.* 101:117-144.
- Reynolds, J. A., E. A. Johnson, and C. Tanford. 1985. Application of the principle of linked functions to ATP-driven ion pumps: kinetics of activation by ATP. *Proc. Natl. Acad. Sci. USA.* 82:3658-3661.
- Simons, T. J. B. 1974. Potassium:potassium exchange catalysed by the sodium pump in human red cells. *J. Physiol.* 237:123-155.
- Simons, T. J. B. 1975. The interaction of ATP-analogues possessing a blocked γ -phosphate group with the sodium pump in human red cells. *J. Physiol.* 244:731-739.
- Smith, R. L., K. Zinn, and L. C. Cantley, Jr. 1980. A study of the vanadate-trapped state of the (Na, K)-ATPase. *J. Biol. Chem.* 255: 9852-9859.
- Sweadner, K. 1989. Isozymes of the $\text{Na}^+/\text{K}^+\text{-ATPase}$. *Biochim. Biophys. Acta.* 988:185-220.
- Wagg, J., M. Holmgren, D. C. Gadsby, F. Bezanilla, R. F. Rakowski, and P. De Weer. 1996. Na/K-pump-mediated charge movements as an assay of Na^+ translocation and occlusion/deocclusion rates. *Biophys. J.* 70: A18 [Abstract].
- Walker, J. F., G. P. Reid, J. A. McCray, and D. R. Trentham. 1988. Photolabile 1-(2-nitrophenyl)ethyl phosphate esters of adenine nucleotide analogues. Synthesis and mechanism of photolysis. *J. Am. Chem. Soc.* 110:7170-7177.
- White, B., and R. Blostein. 1982. Comparison of red cell and kidney $(\text{Na}^+ + \text{K}^+)\text{-ATPase}$ at 0°C. *Biochim. Biophys. Acta.* 688:685-690.
- Wuddel, I., and H.-J. Apell. 1995. Electrogenicity of the sodium transport pathway in the Na, K-ATPase probed by charge-pulse experiments. *Biophys. J.* 69:909-921.